

The Price is Right? How Pricing and Incentive Mechanisms in California Incentivize Building Distributed Hybrid Solar and Energy-Storage Systems

Sushant Varghese

Harold and Inge Marcus Department of Industrial and Manufacturing Engineering, The Pennsylvania State University, 310 Leonhard Building, University Park, Pennsylvania 16802, United States of America

Ramteen Sioshansi*

Department of Integrated Systems Engineering, The Ohio State University, 1971 Neil Avenue, Columbus, Ohio 43210, United States of America

Abstract

Distributed energy resources, including photovoltaic solar and energy storage, are seeing increased deployment. The optimal configuration and operation of these resources depend on several external factors, including energy pricing, incentive programs, and the provision of capacity payments. We model, as a mixed-integer optimization problem, the design and operation of a hybrid energy system that consists of photovoltaic solar arrays that are coupled with energy storage using a shared inverter. We apply our optimization model to a case study that considers two locations in California and a variety of pricing and subsidy regimes. We demonstrate that a well designed time-variant retail tariff provides reasonable incentives for building and operating a hybrid energy system. On the other hand, investment tax credits and the provision of capacity payments can be considerably more distortionary. In particular, constraints that govern the investment tax credit in the United States can hamper significantly the deployment of the hybrid energy systems that we examine.

Keywords: Distributed energy systems, energy pricing, energy policy, capacity value, photovoltaic solar, energy storage

1. Introduction

The past decade has seen significant adoption of photovoltaic (PV) solar arrays, especially at the distribution level. This deployment of PV generation is driven by a number of developments. Two factors are high retail electric rates in some regions and decreases in the installation cost of PV solar arrays, which improve the economic rationale of customers using PV generation to offset grid-supplied energy. The economics of PV generation also benefit in some areas from subsidies or other incentive mechanisms. In the United States, for example, most solar generation facilities are eligible for an investment tax credit (ITC) that is equal to 30% of its capital cost.

A more recent development in deploying distribution-level PV generation is to couple them with other distributed energy resources, such as energy storage. Coupling energy storage with a PV array can offer a number of benefits. One is that energy storage can allow for downsizing the inverter that is used to connect the PV array to the distribution system without increasing the curtailment of solar production. [Denholm and Sioshansi \(2009\)](#) demonstrate such a use of energy storage for downsizing a transmission line that connects a wind generator to a power system. A second benefit of coupling energy storage and a

*Corresponding author

Email addresses: ssv5097@psu.edu (Sushant Varghese), sioshansi.1@osu.edu (Ramteen Sioshansi)

PV array is the ability of the former to shift solar generation to time periods with higher energy prices. [Sioshansi and Denholm \(2010\)](#) show that solar availability tends to be correlated but not perfectly coincident with load and wholesale energy prices in most North American markets. This correlation is because electricity demand is driven primarily by air conditioning load in the summer in these systems. Furthermore, [Denholm et al. \(2015\)](#) show that as the penetration of solar generation increases, peaks in electric net loads and prices can become less correlated and coincident with solar availability. A third benefit of coupling them is that energy storage can increase the capacity value of a PV array, thereby increasing the benefit of the combined system toward power system reliability. [Madaeni et al. \(2013b\)](#) demonstrate such a benefit of integrating thermal energy storage into a concentrating solar thermal power plant. A fourth benefit is that the energy storage can arbitrage differences in wholesale energy prices, although this use of energy storage is independent of (if not impeded by) its co-location with a PV array.

A number of works, including those of [Hoppmann et al. \(2014\)](#); [Mariaud et al. \(2017\)](#); [Weniger et al. \(2014\)](#), examine the techno-economics of coupling distribution-level energy storage and PV generation. [Mariaud et al. \(2017\)](#) develop an integrated model that can be used for technology selection and operational optimization of a distributed energy system in a commercial building that includes energy storage. They use the model to examine the impacts of feed-in tariffs on the economic viability of such a system. [Zhu et al. \(2014\)](#) model energy-flow control in a residential distributed energy system that consists of energy storage and a PV array. Their model is formulated to maximize the benefit of the distributed energy system in reducing the end customer’s energy-supply costs. Based on these results, optimal system designs that meet a budget that is fixed exogenously are determined.

A question that the existing literature does not address well is what affect policy-related distortions may have on the optimal configuration and use of a hybrid energy system. In most instances, retail electricity tariffs drive the design and operation of a hybrid energy system. Retail tariffs are divorced often from wholesale prices, which reflect the real-time marginal cost of supplying energy. As such, wholesale prices reflect the true value of energy that is produced by a hybrid energy system. Retail price tariffs are, in many cases, load-weighted averages of wholesale prices and do not convey this information. As such, the use of retail (as opposed to wholesale) prices can distort the configuration and operation of a hybrid energy system. There are some retail tariffs that include time-variant energy prices. However, the prices in these tariffs often are set *a priori*, which implies that they do not convey the same real-time information that wholesale prices do.

Another operational and configuration inefficiency stems from the solar ITC. Current Internal Revenue Service (IRS) rules allow an energy-storage system that is coupled with a solar generator to receive the ITC under certain circumstances. At least 75% of the energy that is stored must be derived from the solar generator and the ITC rate is prorated depending upon the amount of stored energy that is solar derived (*i.e.*, 100% of the stored energy must be solar-derived for the energy storage to receive the full 30% ITC). Thus, the presence of the ITC imposes constraints on the operation of the energy storage, which may skew the operation and configuration of a hybrid energy system.

[Denholm et al. \(2017\)](#) examine the impacts of the ITC on the operation of a hybrid energy system that consists of energy storage coupled with a PV array. Specifically, they examine the financial impact of the ITC under different coupling cases, which reflect the extent to which the energy storage is restricted in storing only solar-derived energy. However, [Denholm et al. \(2017\)](#) examine only the operational impacts of the ITC. This is because they model a fixed configuration of the PV array, energy storage, and inverters in the hybrid energy system.

Our work in this paper extends the analysis of [Denholm et al. \(2017\)](#). We do this by examining how energy pricing and the ITC and its associated coupling restrictions impact the operation *and* configuration of a hybrid energy system that consists of PV generation and energy storage. We examine also, in two sensitivity cases, the impacts of providing payments to the hybrid energy system that reflect its capacity value and the use of different energy storage technologies. In all of these cases, we model decisions from the perspective of the private investor/owner of the hybrid energy system. By contrasting the optimal operation and configuration under a case with minimal policy distortions to those in cases with price- or ITC-related distortions, we examine how distortionary those policies are.

Using price and weather data for two locations in Southern California, we find that the incumbent utility

(Southern California Edison) provides a time-variant retail rate that overstates the diurnal differences in wholesale prices. As such, the energy storage in the hybrid energy systems that are built at the two locations that are modeled are oversized slightly under retail pricing compared to the socially optimal design that wholesale prices would yield. Moreover, the hybrid energy systems earn considerably higher profits under retail pricing relative to wholesale pricing. We find also that the ITC and its associated coupling restrictions limit significantly the potential use of energy storage in a hybrid energy system. Thus, if the goal of extending the ITC to energy storage is to incentivize its use, the current policy does not appear to be designed well. Capacity payments provide strong incentives for the deployment of energy storage, which in most cases overcome the limitations that are imposed by the coupling restrictions of the ITC. Although the amounts of energy storage that are deployed in the presence of capacity payments are closer to the minimal-distortion case, the energy storage still is used inefficiently (due to the ITC’s coupling restriction). We find also that the optimal designs and operations of the hybrid energy systems are similar qualitatively for most energy storage technologies.

The remainder of this paper is organized as follows. Section 2 provides an overview of how we assume the hybrid energy system is designed and a detailed formulation of the model that is used to optimize its design and operation. Appendix A provides further technical details on how the optimization model is linearized. Section 3 details the data that are used in our case study. Sections 4 and 5 discuss our case study and sensitivity analysis results, respectively. Section 6 provides a discussion of our findings and concludes.

2. Model

We begin in this section by giving an overview of the hybrid energy system that we model. Then, we introduce model notation and detail the model formulation. The model includes some nonlinearities, which arise from the ITC and the calculation of the capacity value of the system. Appendix A provides details on how these are approximated linearly, using binary expansion, which yields a tractable mixed-integer linear optimization problem.

2.1. System Architecture and Model

Following the work of Denholm et al. (2017), we model the system that is illustrated in Figure 1. It consists of a distribution circuit with a fixed capacity in which a PV array with a fixed capacity is installed. The PV array must be connected to the distribution circuit using an inverter, the size of which is determined in the model. Moreover, the PV array can be co-located with a battery-energy-storage system (*i.e.*, the PV array and battery share the same inverter to connect to the power system). The power and energy capacities of the battery also are determined in the model. The system is designed (*i.e.*, the inverter and battery sizes are determined) to maximize the net profit that the system earns from market transactions. Revenues are earned from energy transactions and the provision of capacity to the power system. The distributed-energy system incurs capital costs for installing the PV array, inverter, and battery. These costs are annualized so they are comparable to the revenues, which are modeled over a limited optimization horizon (which is taken to be a year in our case studies). Depending on how the system is designed and operated, the capital costs may be eligible also for an ITC.

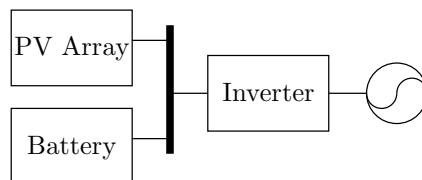


Figure 1: Schematic Diagram of Hybrid Energy System

2.2. Model Notation

2.2.1. Indices, Parameters, and Sets

C^C	annualized capital cost of a conventional capacity resource [\$/kW-year]
C^E	annualized capital cost of battery energy capacity [\$/kWh-year]
C^I	annualized capital cost of inverter [\$/kW-year]
C^P	annualized capital cost of battery power capacity [\$/kW-year]
C^{PV}	annualized capital cost of PV array [\$/year]
\bar{K}	distribution-circuit capacity [kW]
\bar{P}_t^{PV}	hour- t PV output available [kW]
r_t	hour- t energy price [\$/kWh]
T	set of hours in optimization horizon
t	index for hours
η^C	charging efficiency of battery [p.u.]
η^D	discharging efficiency of battery [p.u.]
$\Xi(\cdot)$	function relating the capacity value of the battery to its energy capacity [p.u.]
ξ^{PV}	capacity value of PV array [kW]

Our model considers a set, T , of hours over which the configuration and operation of the distributed-energy system are optimized. Because the capacity of the PV array is fixed, we model its capital cost, C^{PV} , as being fixed as well. Conversely, the costs of the inverter and battery scale linearly based on their sizes. The battery is modeled as having two cost components— C^E represents the cost of increasing the energy-carrying capacity of the battery whereas C^P represents the cost of increasing its power capacity.

Following the work of [Denholm et al. \(2017\)](#), we assume that the capital cost of a conventional capacity resource, C^C , is used to determine the capacity payments that the distributed-energy system earns. This capacity payment depends on the capacity value of the PV array and battery. As [Madaeni et al. \(2013a\)](#) show, the former is fixed, inasmuch as it depends on the size, location, and orientation of the PV array, all of which are assumed to be fixed. [Sioshansi et al. \(2014\)](#) show that the capacity value of the battery depends on its energy and power capacities. $\Xi(\cdot)$ is a function that relates the capacity value, which is measured on a p.u. basis relative to the power capacity of the battery, to its energy capacity.

2.2.2. Decision Variables

\bar{B}^E	battery energy capacity [h]
\bar{B}^P	battery power capacity [kW]
\bar{I}	inverter capacity [kW]
P_t^C	hour- t battery-charging power from the power system [kW]
P_t^D	hour- t battery-discharging power [kW]
P_t^N	hour- t net power exports to the power system [kW]
$P_t^{PV,C}$	hour- t PV output that is used to charge the battery [kW]
$P_t^{PV,X}$	hour- t PV output that is exported to the power system [kW]
s_t	ending hour- t state of charge (SOC) of battery [kWh]
ξ^S	capacity value of distributed-energy system [kW]
τ	investment tax credit rate [p.u.]

\bar{B}^P represents the charging and discharging power capacities (which are equal to one another) of the battery in kW, whereas \bar{B}^E represents its energy capacity in hours. This means that the SOC of the battery can reach at most $\bar{B}^E \bar{B}^P$. The output of the PV system is decomposed into two terms. $P_t^{PV,C}$ represents hour- t PV output that is used to charge the battery while $P_t^{PV,X}$ represents output that is exported (sold) to the power system.

2.3. Model Formulation

Our model is formulated as:

$$\max C^C \xi^S + \sum_{t \in T} r_t P_t^N - (1 - \tau) (C^I \bar{I} + C^E \bar{B}^E \bar{B}^P + C^P \bar{B}^P + C^{\text{PV}}) \quad (1)$$

$$\text{s.t. } P_t^N = P_t^{\text{PV},X} + P_t^D - P_t^C \quad \forall t \in T \quad (2)$$

$$- \bar{I} \leq P_t^N \leq \bar{I} \quad \forall t \in T \quad (3)$$

$$- \bar{K} \leq P_t^N \leq \bar{K} \quad \forall t \in T \quad (4)$$

$$P_t^{\text{PV},C} + P_t^{\text{PV},X} \leq \bar{P}_t^{\text{PV}} \quad \forall t \in T \quad (5)$$

$$P_t^{\text{PV},C}, P_t^{\text{PV},X} \geq 0 \quad \forall t \in T \quad (6)$$

$$s_t = s_{t-1} + \eta^C \cdot (P_t^C + P_t^{\text{PV},C}) - P_t^D / \eta^D \quad \forall t \in T \quad (7)$$

$$0 \leq s_t \leq \bar{B}^E \bar{B}^P \quad \forall t \in T \quad (8)$$

$$0 \leq P_t^C + P_t^{\text{PV},C} \leq \bar{B}^P \quad \forall t \in T \quad (9)$$

$$0 \leq P_t^D \leq \bar{B}^P \quad \forall t \in T \quad (10)$$

$$\xi^S \leq \bar{I} \quad (11)$$

$$\xi^S \leq \bar{K} \quad (12)$$

$$\xi^S \leq \xi^{\text{PV}} + \Xi(\bar{B}^E) \bar{B}^P \quad (13)$$

$$\sum_{t \in T} P_t^{\text{PV},C} \geq 0.75 \sum_{t \in T} (P_t^C + P_t^{\text{PV},C}) \quad (14)$$

$$(1 - \tau) \sum_{t \in T} (P_t^C + P_t^{\text{PV},C}) = \sum_{t \in T} (P_t^C + P_t^{\text{PV},C}) - 0.3 \sum_{t \in T} P_t^{\text{PV},C}. \quad (15)$$

Objective function (1) computes system profits, which consists of three terms. The first is the capacity payment that the system receives, which depends upon its rated capacity value and the annualized cost of a conventional capacity resource. The second term is the revenue that is earned from energy transactions. The third is the capital cost of the system, taking into account any ITC that is earned.

The model has five sets of constraints. The first, (2)–(4) pertains to energy balance within the system and energy transactions with the power system. Constraints (2) impose hourly energy balance on the hybrid energy system. Constraints (3) and (4) impose limits, based on the inverter and circuit capacities, on the amount of power that is exchanged with the power system. Because the battery and PV array are co-located and share the same inverter, \bar{I} imposes a limit on the total amount of power that can be imported to or exported from the two of them together.

Constraints (5) and (6) pertain to the operation of the PV system. Constraints (5) ensure that the total amount of power output from the PV array in each hour does not exceed the available power. Constraints (6) impose non-negativity on the PV array's output.

Constraints (7)–(10) pertain to the operation of the battery. Constraints (7) give the hourly evolution of the SOC of the battery. Constraints (8) impose the SOC limits, whereas (9) and (10) impose charging and discharging power limits, respectively. Some energy storage models, including the works of [Bienstock et al. \(2017\)](#); [Sakti et al. \(2017\)](#), include restrictions that prohibit the energy-storage system from charging and discharging simultaneously. We do not include such an explicit constraint, as charging and discharging the battery simultaneously is suboptimal typically (due to the inherent energy losses). Binary variables could be added to our model to impose such a restriction, however.

Constraints (11)–(13) define the capacity value of the distributed-energy system. The contribution of the distributed-energy system to power system reliability is limited by its ability to export energy. Constraints (11) and (12) impose these limits by limiting ξ^S to be no greater than either of \bar{I} or \bar{K} . The capacity value is limited also by the ability of the system to provide energy during peak-load periods. [Denholm et al. \(2017\)](#) note that this ability depends upon the configuration of the PV array and battery. The PV array

provides a fixed capacity value, ξ^{PV} . The battery provides capacity value that depends upon its configuration. Sioshansi et al. (2014) show how the energy capacity of an energy-storage system affects its capacity value. The term, $\Xi(\bar{B}^E)\bar{B}^P$, in (13) captures this impact.

The final two constraints pertain to administrative rules that govern the ITC.¹ Constraint (14) imposes a restriction that for an hybrid energy system that consists of solar generation and energy storage to be eligible for the ITC, solar generation must provide at least 75% of the energy that is used to charge the energy-storage system. Constraint (15) imposes the prorating of the ITC, which is based on how much of the energy that is used to charge the energy-storage system is provided by solar generation. If solar generation provides all of the charging energy, then:

$$\sum_{t \in T} (P_t^C + P_t^{\text{PV},C}) = \sum_{t \in T} P_t^{\text{PV},C},$$

and (15) simplifies to $\tau = 0.3$, meaning that the system receives the full 30% ITC. Otherwise, if:

$$\sum_{t \in T} (P_t^C + P_t^{\text{PV},C}) > \sum_{t \in T} P_t^{\text{PV},C},$$

the ITC is prorated linearly.

3. Case Study Data

Our case study considers two locations, the characteristics of which are summarized in Table 1, in the year 2015. Los Angeles is an urban area that is highly conducive to the deployment of rooftop PV arrays. Moreover, Los Angeles is a load pocket, meaning that transmission constraints may yield relatively high locational marginal prices (LMPs), potentially increasing the value of PV production. Mojave, conversely, is a rural area that may not have the same transmission-related impacts on its LMPs. Indeed, the simple-average of the LMPs for Mojave in 2015, which are obtained from California Independent System Operator (CAISO), are about 5% lower than that for Los Angeles.

Table 1: Characteristics of Locations Modeled

Location	Coordinates	Average Daily Global Horizontal Irradiation [kWh/m ² /day]	Wholesale Price Point
Los Angeles, California	34.05° N, 118.25° W	5.39	GOULD_2_N007
Mojave, California	35.01° N, 115.46° W	5.78	CIMA_2_N101

We model the system under three operational regimes, which we term flexible, prorated, and tight coupling. These regimes are related to how the ITC constrains the operation of the energy storage. Under flexible coupling, which assumes that the hybrid energy system does not receive the ITC, there is complete flexibility to charge the energy storage using PV-derived or grid energy. Flexible coupling is modeled by relaxing (14) and (15) and fixing τ equal to zero in the model. Prorated coupling allows grid energy to be charged into the energy storage, however we impose current IRS rules that require that at least 75% of the charging energy be obtained from the PV array to maintain eligibility for the ITC. Moreover, the ITC rate is prorated under prorated coupling, depending on how much PV energy is used for charging. Constraints (14) and (15) impose these rules. Under tight coupling, only PV-derived energy can be stored. This case is modeled by relaxing (14) and (15), fixing τ equal to 0.3, and imposing non-negativity constraints on the P_t^N 's (which prevents the hybrid energy system from importing energy from the grid for charging energy storage).

¹<https://www.irs.gov/pub/irs-wd/1308005.pdf>

We model hourly energy production of the PV array in each location using meteorological data from the National Solar Radiation Database (NSRDB). [Sengupta et al. \(2018\)](#) describe the NSRDB, which is a serially complete collection of half-hourly values of meteorological data. The data are produced using a physics-based approach that is detailed by [Sengupta et al. \(2014a,b\)](#). [Habte et al. \(2017\)](#) validate the performance of the dataset. The NSRDB data for each location, which are converted to hourly observations, are processed using System Advisor Model (SAM). [Blair et al. \(2014\)](#) provide a general description of SAM, which simulates the hourly net electric output of a solar system, given fixed system parameters and meteorological data. Each PV array that we model has a 6-kW nameplate capacity, which is the average size of distributed PV installations in the United States.² The panel and inverter types are set to the default values in SAM. The PV panel is assumed to cost \$2490/kW, based on data that are reported by [Fu et al. \(2018\)](#), and a fixed orientation with a 180° azimuth and 20° tilt. Table 1 shows that Mojave has slightly higher average daily global horizontal irradiation, which translates into approximately 10.7% greater solar production over the year compared to Los Angeles.

We assume a 33-kW distribution circuit, which is in the range of typical residential service ratings. Thus, we do not consider demand charges or other fees that could be incurred by a larger circuit. Table 2 summarizes the technical characteristics of the six energy storage technologies—vanadium redox (VRB), lead-acid (PbA), zinc-bromine (ZNBR), polysulfide bromide (PSB), sodium-sulfur (NaS), and Li-ion batteries—that we consider. The technical characteristics are based on values that are reported by [Aneke and Wang \(2016\)](#); [Arbabszadeh et al. \(2017, 2019\)](#); [Cole et al. \(2016\)](#); [Dunn et al. \(2011\)](#); [Eyer and Corey \(2010\)](#); [Gallo et al. \(2016\)](#); [Kintner-Meyer et al. \(2012\)](#); [Kyriakopoulos and Arabatzis \(2016\)](#); [Schmidt et al. \(2017\)](#); [Schoenung \(2011\)](#); [Zafraakis et al. \(2016\)](#); [Zakeri and Syri \(2015\)](#).

Table 2: Characteristics of Energy Storage Technologies

Technology	Round-Trip Efficiency [p.u.]	Lifetime [years]	Investment Cost	
			Energy [\$/kWh]	Power [\$/kW]
VRB	0.95	15	150	398
PbA	0.90	15	200	222
ZNBR	0.75	10	150	178
PSB	0.85	15	120	330
NaS	0.90	15	180	250
Li-ion	0.90	15	320	620

The cost of the inverter that connects the hybrid energy system to the power system depends upon the energy-storage technology that is built and the operational regime (*i.e.*, flexible, prorated, or tight coupling) that is being modeled. Under flexible or prorated coupling, the hybrid energy system requires a bidirectional inverter, which allows bidirectional energy exchange with the power system. The power-related investment costs that are given in Table 2 represent the cost of the battery inverter. Thus, we model these cases by setting C^P equal to the value in Table 2 that corresponds to the technology being modeled and C^I equal to zero (as C^P represents the full inverter cost). We add the constraint:

$$\bar{B}^P = \bar{I},$$

which fixes the power capacity of the battery equal to the inverter capacity in the model when modeling flexible or prorated coupling.

Under tight coupling (or in a case in which energy storage is not built), the hybrid energy system requires only a unidirectional inverter. This is because in these cases power cannot flow from the power system to the hybrid energy system. Based on data that are reported by [Fu et al. \(2018\)](#), we model these cases assuming a

²<https://news.energysage.com/average-solar-panel-size-weight/>

\$210/kW inverter cost. In all cases, we assume that the battery has a starting SOC of zero at the beginning of the optimization horizon.

Following the work of [Denholm and Sioshansi \(2009\)](#), we annualize the capital costs of the PV array, inverter, and energy-storage system by the factor:

$$\frac{\gamma}{1 - (1 + \gamma)^{-\lambda}},$$

where λ is the lifetime of the asset and γ is the discount rate, which we take to be 11%. We take the PV array and inverter to have 25- and 22-year lifetimes, respectively.

We use two sets of energy prices in (1). The first are the historical LMPs from the year 2015 for the price points that are listed in Table 1, which are obtained from CAISO. The second are time-varying retail prices that are offered by Southern California Edison, which is the incumbent electric utility in Southern California, under Tariff TOU-D-A.³ These retail prices are the same for both locations.

We model the capacity value of the hybrid energy system as depending on its configuration in three ways. First, the capacities of the distribution circuit and inverter impose upper bounds on the amount of power that the hybrid energy system can inject into the power system. This relationship is enforced by (11) and (12). Second, the PV array provides capacity value, which we estimate as being 40% of its nameplate capacity. Third, depending on its configuration, the energy storage also can provide capacity value. We model the capacity value of the energy storage as being a multiplicative factor, $\Xi(\bar{B}^E)$, of its power capacity. Table 3 gives the relationship between \bar{B}^E and $\Xi(\bar{B}^E)$ that we use, which is taken from the work of [Sioshansi et al. \(2014\)](#). We apply piecewise linear interpolation between the breakpoints that are given in the table. Following the work of [Denholm et al. \(2017\)](#), the capacity value of the hybrid energy system is monetized into a capacity credit using the annualized cost of a natural gas-fired combustion turbine, which is assumed to be \$149/kW-year.

Table 3: Relationship Between Energy Capacity and Capacity Value of Energy Storage

\bar{B}^E	$\Xi(\bar{B}^E)$
0	0.00
1	0.41
2	0.67
4	0.92
≥ 6	0.95

4. Case Study Results

We conduct our case study by examining the financial cases that are summarized in Table 4, assuming no capacity payments for the hybrid energy system (*i.e.*, we fix $C^C = 0$ and focus solely on the impact of energy prices and the ITC on the configuration of the system). We examine the impacts of capacity payments as a sensitivity analysis in Section 5.1. We label the first case in Table 4 the Base Case, inasmuch as there is minimal policy intervention in the configuration of the hybrid energy system. This is because wholesale LMPs reflect the system marginal value of energy and there are no subsidies or ITC-related constraints on the operation of the battery in the Base Case. Contrasting the Base Case with the other five cases that are in Table 4 allows us to discern how different policy interventions impact the privately optimal configuration of the hybrid energy system.

Figure 2 summarizes the operation of the hybrid energy system in Los Angeles on 1 January in the Base Case. The figure assumes no capacity payments and that VRB energy storage, which achieves the highest

³<https://www.sce.com/residential/rates/sce-grandfathered-rate-plans>

Table 4: Financial Cases That Are Examined in Section 4

Case	Energy Prices	Coupling	ITC
Base	Wholesale	Flexible	No
Retail Flexible	Retail	Flexible	No
Wholesale Prorated	Wholesale	Prorated	Prorated
Retail Prorated	Retail	Prorated	Prorated
Wholesale Tight	Wholesale	Tight	Yes
Retail Tight	Retail	Tight	Yes

profits among the battery technologies that we consider, is built. The impact of using other energy storage technologies is summarized in Section 5.2. The figure shows that solar output peaks in the middle of the day but is not coincident with the peak in energy prices, which occur later in the evening. As such, the battery is used to store most of the energy that is produced by the PV array, which is sold back to the power system later when energy prices peak. Indeed, because of the flexible coupling in the Base Case, the battery is charged with considerably more energy midday than what the PV array produces, meaning that the hybrid energy system is a net purchaser of energy during these hours (the PV array produces a total of 25.8 kWh during the day between hours 8 and 17 but the battery stores a total of 231.0 kWh during these hours). The battery charges an additional 109.3 kWh in the early morning, before any PV production. These operating patterns persist over the year, with the hybrid energy system shifting an average of about 300 kWh daily in the Base Case to exploit diurnal price differences, despite the PV array producing an average of only 27.3 kWh daily.

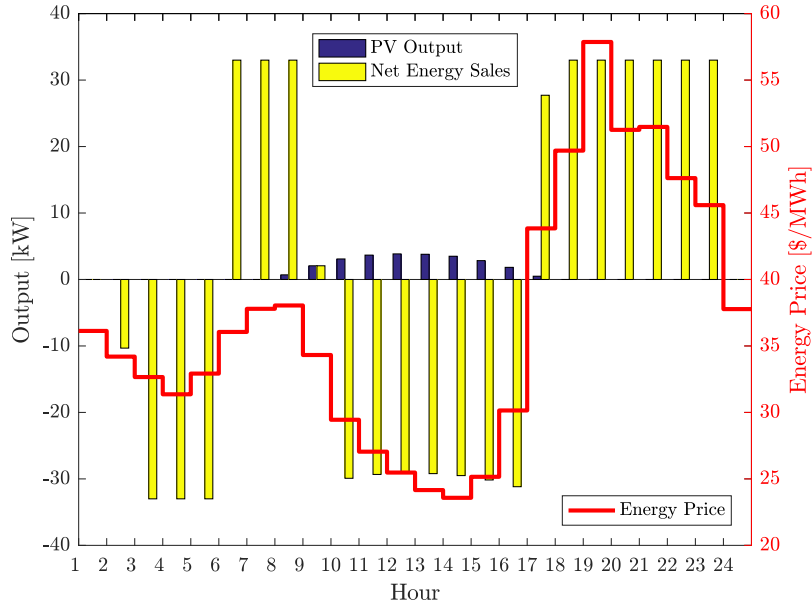


Figure 2: Operation of Hybrid Energy System With VRB Energy Storage in Los Angeles on 1 January, 2015 in Base Case

Figure 3 shows the operation of the hybrid energy system with VRB energy storage and no capacity payments on the same day in the Wholesale Tight Case. Because of the restriction in this case that it be charged only with PV-produced energy, the battery charges only 25.8 kWh in the middle of the day, which is sold in hour 19, when the price is at its peak. The restriction on using PV-produced energy only results in the battery charging an average of 23.8 kWh of energy daily over the course of the year that is modeled.

Table 5 summarizes the optimal configurations and profits of the hybrid energy systems that are built

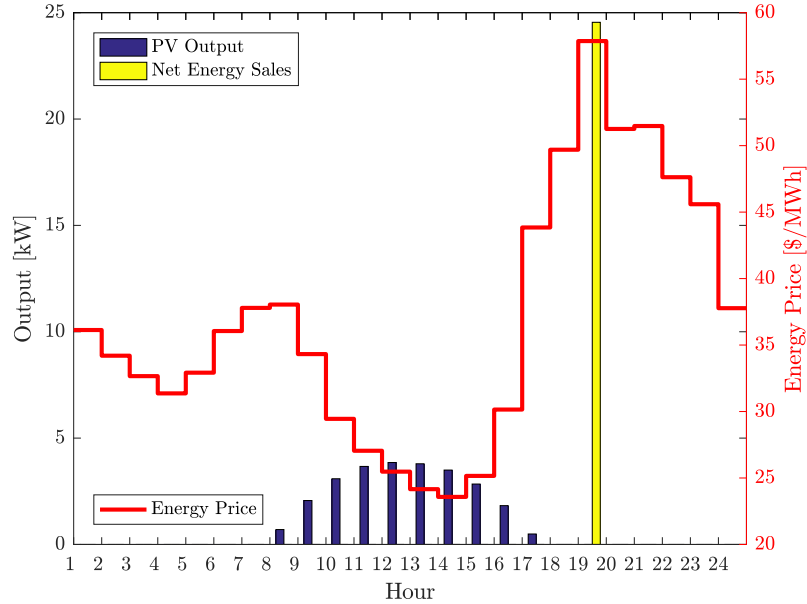


Figure 3: Operation of Hybrid Energy System With VRB Energy Storage in Los Angeles on 1 January, 2015 in Wholesale Tight Case

with VRB energy storage and no capacity payments in Los Angeles in the six financial cases that are summarized in Table 4. Table 5 shows that the configuration of the hybrid energy system is highly sensitive to its financial treatment. The Base and Retail Flexible Cases, in which there are no ITC-related constraints on the configuration or operation of the hybrid energy system, result in significantly different configurations compared to the other cases. In the Base and Retail Flexible Cases the hybrid energy system earns profits primarily from energy arbitrage. As such, the inverter capacity is constrained solely by the 33-kW capacity of the distribution circuit.

Table 5: Optimal Configurations and Profits of Hybrid Energy Systems With VRB Energy Storage in Los Angeles

Case	Configuration		Annual Profit [\$ thousand]	Operating Profit [% of Solar-Only]
	$\bar{I} = \bar{B}^P$	\bar{B}^E		
Base	33.0	7	9.2	474.7
Retail Flexible	33.0	10	14.9	846.5
Wholesale Prorated	28.6	1	2.7	86.4
Retail Prorated	6.9	6	2.1	65.9
Wholesale Tight	25.8	1	2.7	57.1
Retail Tight	4.7	6	1.8	32.2

The final column of Table 5 demonstrates how much energy arbitrage impacts the hybrid energy system in the six different cases. It summarizes the increase in operating profits that the hybrid energy systems earn from having energy storage compared to a no-storage case in which profits are earned solely from selling PV output. This is computed as:

$$\frac{\sum_{t \in T} r_t \cdot (P_t^N - \bar{P}_t^{\text{PV}})}{\sum_{t \in T} r_t \bar{P}_t^{\text{PV}}}.$$

This column of the table reinforces further the hybrid energy system being configured and operated in

a vastly different manner in the Base and Retail Flexible Cases compared to the others. With the ITC imposed, the hybrid energy system is limited greatly in its ability to profit from energy arbitrage. This limitation is especially true in the Retail Tight Case, as energy storage can be used only to shift PV output around in time and allow the inverter to be undersized relative to the PV array. In the prorated cases, 25% of the energy that is used to charge the battery is derived from the grid (which is the limit allowed under IRS regulations). As such, the hybrid energy system receives a reduced 22.5% ITC, as opposed to the full 30% ITC if only PV-derived energy is used to charge the battery. This means that the incremental revenue that is earned from being able to arbitrage diurnal price differences outweighs the increased capital costs that stem from a lower ITC. Conversely, without the ITC, having access to energy storage gives considerable operating-profit increases in the Base and Retail Flexible Cases.

Table 5 shows that \bar{B}^E is greater in the Retail Flexible Case compared to in the Base Case, yielding higher profits. This means that retail prices under Tariff TOU-D-A overstate the value of shifting energy between low- and high-price periods relative to the true system value of energy arbitrage that is reflected in wholesale prices. Indeed, the volume-weighted average price at which the hybrid energy system purchases energy with which to charge the battery in the Base Case is \$25.28/MWh, as opposed to \$12.67/MWh in the Retail Flexible Case. The volume-weighted average price at which the hybrid energy system sells energy in the Base Case is \$40.14/MWh, as opposed to \$32.67/MWh in the Retail Flexible Case. This greater price spread of \$20.01/MWh in the Retail Flexible case (compared to \$14.86/MWh in the Base Case) results in the hybrid energy system shifting an average of 330 kWh of energy daily as opposed to only 300 kWh in the Base Case.

In the cases with the ITC (*i.e.*, the cases with prorated and tight coupling), the battery is configured with much higher power capacity under wholesale as compared to retail pricing (although the energy-carrying capacities of the batteries are comparable between the two pricing regimes). This is because wholesale prices can have more extreme peaks compared to retail prices, which can be exploited if the battery has a high power capacity. Wholesale pricing yields higher profits also. This is because with the ITC, (14) limits the amount of energy arbitrage that the battery can engage in using grid-sourced energy. Instead, the battery is used primarily to shift PV output to higher-priced periods of the day. Although retail prices have a larger spread between on- and off-peak prices, wholesale on-peak prices are greater. As such, wholesale pricing increases the value proposition of energy storage with ITC-related operating constraints.

Table 6 summarizes the optimized configurations and operations of the hybrid energy systems in Mojave under the same set of financial cases that are in Table 4. As in Table 5, these configurations assume no capacity payments and the use of VRB. The results that are summarized in Table 6 are qualitatively similar to those that are summarized in Table 5, with the exception of the Wholesale Prorated Case. In addition to having lower average LMPs than Los Angeles, the spread between on- and off-peak wholesale prices at Mojave is smaller than it is at Los Angeles. The average difference between the daily maximum and minimum LMPs in Mojave is \$26.84/MWh, as opposed to \$30.33/MWh in Los Angeles. Given these smaller price spreads, there is less financial value in having a high-power battery to exploit peaks in the price pattern. Rather, under wholesale pricing, it is preferable to build an energy-storage system with lower power but similar energy-carrying capacities. Despite the lower average wholesale prices in Mojave, the hybrid energy system earns slightly higher profits in the Wholesale Prorated Case (compared to in Los Angeles), due to greater solar production.

In the Wholesale Tight Case, high-power batteries are built in both Mojave and Los Angeles. A high-power battery is optimal in Mojave in the Wholesale Tight Case because under tight coupling a unidirectional inverter (with relatively low power-capacity costs) can be built. Such a battery can exploit profitably the relatively smaller differences in on- and off-peak wholesale prices at Mojave. These similarities in the system configurations mean that wholesale versus retail pricing and the availability of the ITC impact the configuration and operation of the hybrid energy system in Mojave much the same as they do those in Los Angeles. The battery systems that are deployed in Mojave with the ITC are larger than those in Los Angeles. This is because the PV array in Mojave produces more energy than a comparable system in Los Angeles does. As such, more energy can be stored without violating (14). As in Los Angeles, it is optimal for the hybrid energy system in Mojave to derive the full 25% of its charging energy from the grid that (14) allows in the two cases with prorated coupling. This yields a 22.5% ITC in these two cases.

Table 6: Optimal Configurations and Profits of Hybrid Energy Systems With VRB Energy Storage in Mojave

Case	Configuration		Annual Profit [\$ thousand]	Operating Profit [% of Solar-Only]
	$\bar{I} = \bar{B}^P$	\bar{B}^E		
Base	33.0	7	8.5	448.1
Retail Flexible	33.0	10	15.1	786.9
Wholesale Prorated	7.8	6	2.8	72.8
Retail Prorated	7.7	6	2.5	70.9
Wholesale Tight	29.0	1	2.7	61.4
Retail Tight	5.3	6	2.1	36.1

Although average wholesale prices in Mojave are lower than they are in Los Angeles, wholesale prices yield higher profits in Mojave (compared to in Los Angeles) in the presence of the ITC. This is because the PV array in Mojave produces more energy than the PV array in Los Angeles does. Thus, the greater volume of energy that is produced in Mojave outweighs the lower prices at which it is sold. Conversely, in the Base Case, in which most of the profits are earned from energy arbitrage, the hybrid energy system earns less profit in Mojave compared to Los Angeles, due to the lower wholesale prices in Mojave.

5. Sensitivity Analyses

This section presents the results of two sensitivity analyses. We examine first the impact of including capacity payments and second the impact of using different battery technologies on the optimal configuration and operation of the hybrid energy system.

5.1. Capacity Payments

Table 7 summarizes the optimal configurations, profits, and operations of the hybrid energy systems that are built in Los Angeles under the different financial cases when capacity payments are included. The table assumes that VRB energy storage is built. Contrasting Tables 5 and 7 shows that the hybrid energy systems have significantly different configurations in the presence of capacity payments. In all of the financial cases, the inverter and battery are sized to maximize the capacity value of the hybrid energy system. In the Base, Retail Flexible, and Wholesale Tight Cases the battery is sized to have sufficient energy capacity to achieve a near-100% capacity value. The battery is configured differently in the two prorated cases, whereby it has an extremely high power capacity compared to the inverter but only one hour of energy-carrying capability. As such, the battery in this case has only a 41% capacity rating. Nevertheless, because of its high power capacity, the battery has still the same capacity value (in kW) as in the other financial cases (*i.e.*, the 75-kW power capacity of the battery can be ‘spread’ over a full hour to achieve a 31-kW capacity value). This configuration arises in the prorated cases because energy storage has relatively low energy arbitrage value (the ITC limits the volume of energy that can be arbitrated). As such, the battery is sized to emphasize power as opposed to energy-carrying capacity, because of the relatively low power-capacity cost of VRB energy storage.

The hybrid energy systems are operated differently in the presence of a capacity payment. For instance, in the Wholesale Tight Case, the amount of energy that is charged into the battery is increased by about 11.7%, which results in a 11.8% increase in revenues from energy transactions, relative to not having capacity payments. This is due to the larger storage that is built with capacity payments. In the Base Case however, there is no difference in the way the system is configured or operates.

The hybrid energy systems in Mojave are configured and operated similarly to those in Los Angeles. As such, results for Mojave are excluded for sake of brevity.

Table 7: Optimal Configurations, Profits, and Operations of Hybrid Energy Systems With VRB Energy Storage in Los Angeles with Capacity Payments

Case	Configuration		Annual Profit [\$ thousand]	Capacity Value of Battery [kW]
	$\bar{I} = \bar{B}^P$	\bar{B}^E		
Base	33.0	7	14.1	31.4
Retail Flexible	33.0	10	19.8	31.4
Wholesale Prorated	74.6	1	5.9	30.6
Retail Prorated	74.6	1	4.4	30.6
Wholesale Tight	33.0	6	5.5	31.4
Retail Tight	33.0	6	4.1	31.4

5.2. Battery Technology

Table 8 summarizes the optimal configurations, profits, and operations of the hybrid energy systems that are built in Los Angeles using different battery technologies (as well as in a no-battery case). It assumes the financial Base Case with wholesale energy prices, no ITC, flexible coupling, and no capacity payments. The table shows that the optimal configurations of all of the battery technologies are fairly similar. Moreover, the installation of the battery system has a similar impact in terms of being able to profit from storing low-price energy that subsequently is discharged and sold during high-price hours. Although these system configurations are all similar, the profits that are earned by the system varies depending upon the battery technology that is used. This is, in part, because of the different costs of the battery technologies, but also due to their varying round-trip efficiencies. For instance, a ZNBR battery has a relatively low installation cost but also a low round-trip efficiency. As such, a ZNBR battery stores noticeably less energy daily, because the differences between the prices at which energy is discharged and charged must be larger to justify the use of the battery. Although less energy is charged if ZNBR technology is used, a ZNBR battery gives rise to greater energy losses compared to the other technologies (20.3 MWh over the year for a ZNBR battery as opposed to 5.4 MWh–13.8 MWh for the other battery technologies).

Table 8: Optimal Configurations, Profits, and Operations of Hybrid Energy Systems in Los Angeles Under Base Financial Case Using Different Battery Technologies

Technology	Configuration		Annual Profit [\$ thousand]	Average Daily Energy Stored [kWh]	Average Energy-Transaction Price [\$/MWh]	
	$\bar{I} = \bar{B}^P$	\bar{B}^E			Purchases	Sales
No Storage	4.5	n/a	0.8	n/a	n/a	26.68
VRB	33.0	7	9.2	301.0	25.28	40.14
PbA	33.0	6	7.0	261.3	24.86	41.24
ZNBR	33.0	6	3.0	222.4	24.35	43.68
PSB	33.0	6	7.0	246.9	24.68	42.19
NaS	33.0	6	7.4	261.3	24.86	41.24
Li-ion	33.0	6	2.1	261.2	24.86	41.24

The system configurations in Mojave are qualitatively similar to those in Los Angeles, and are excluded for sake of brevity.

6. Conclusion and Policy Implications

We develop a modeling framework that can be used to determine the optimal configuration of a hybrid energy system that includes a PV solar array and energy storage. The model could be used by a potential

investor to size a hybrid energy system. However, our interest is in examining how energy pricing, capacity payments, and the ITC impact incentives for such private investments. Depending upon the financial case that is considered and the imposition of ITC-related constraints and subsidies, energy storage has four potential uses (which may be combined in different cases). One is downsizing the inverter with minimal impacts on the curtailment of solar production. A second is shifting PV production to higher-priced periods. A third is to increase the capacity value of the hybrid energy system. A fourth is to arbitrage diurnal price differences (by buying energy from the power system).

We find that with minimal policy intervention (*i.e.*, in the financial Base Case), the optimal design of the hybrid energy system focuses on using energy storage for energy arbitrage. Including capacity payments does not change substantively the configuration of the system in the financial Base Case, but increases the net profit of the system by over 50%. Depending upon utility-planning practice and the technical capabilities of the power electronics and inverter that connect the hybrid and distribution systems to one another, capacity payments may be distortionary. This is because the power electronics and inverters in most distributed energy systems are designed currently to disconnect from the grid if there is a frequency or voltage excursion. The rationale of this design is that frequency or voltage excursions indicate a power system failure (*e.g.*, a blackout or brownout condition). Disconnecting the distributed energy system reduces the risk of utility crews that are working to restore electricity service being electrocuted by an energized distribution circuit. However, this design choice means that the hybrid energy system disconnects (and stops supplying energy) when the power system is in a contingency condition. Thus, providing capacity payments under such a setting would be compensating the hybrid energy system for a service that it does not provide fully. Inverter and power-electronics designs and utility-planning practice are evolving, however, to make better use of distributed energy resources. [Chang et al. \(2014\)](#) examine such use of distributed energy storage in the state of Texas. Thus, as these technical and utility-practice impediments to having the hybrid energy system improve power system reliability are resolved, the provision of capacity payments is increasingly appropriate.

The hybrid energy system facing retail as opposed to wholesale prices has small impacts (relative to other comparative statics that we examine) on its design and operation. The changes in the system configuration mainly are to take advantage of peaks in wholesale-price patterns. Moreover, these changes provide only marginal profit increases and are dependent on the extent to which wholesale prices have extreme peaks. The limited impact of retail pricing is exactly because we consider a time-variant tariff. There are many time-invariant retail tariffs (or time-variant tariffs that have poor time synchronization with wholesale price patterns), which we do not analyze. Presumably, such tariffs would provide exceedingly poor incentives for the design and deployment of the hybrid energy system. Absent capacity payments, the ITC (under both tight and flexible coupling) has a much more significant impact on the design and operation of the hybrid energy system than retail pricing does. If the goal of extending the ITC to energy storage that is coupled with a solar generator is to incentivize greater deployment and use of energy storage, our results suggest that the policy has a poor design. This is especially true in the tight-coupling cases, in which the energy storage is used for limited shifting of solar generation to higher-priced periods and (in some cases) to downsize slightly the capacity of the inverter. Including capacity payments, even with the ITC, yields hybrid energy system designs that are closer to those that are obtained in the financial Base Case. However, the energy storage is used inefficiently with the ITC. This is because the energy storage is sized to yield capacity payments but it is not used to arbitrage price differences (as is done in the financial Base Case).

Our model and analysis neglect some pricing and incentive mechanisms that may impact the hybrid energy system. Our analysis assumes that wholesale prices can ‘reach’ the hybrid energy system. We assume this because our focus in modeling the financial Base Case is to examine a counterfactual, wherein the design and operation of the hybrid energy system have minimal policy distortion. Wholesale prices without any ITC-related constraints on the operation of energy storage reflect minimal policy distortion, inasmuch as wholesale prices reflect the marginal value of energy to the system. In reality, a distributed energy resource may not have access to tariffs that expose it to wholesale LMPs. Moreover, transmission- and/or distribution-network access fees, taxes, and other costs may be levied on distributed energy resources. Given that the focus of our modeling wholesale prices is to contrast them with retail tariffs in incentivizing the design and operation of the hybrid energy system, these ancillary fees should not be included in modeling

cases with wholesale prices. Conversely, if one is conducting a detailed financial analysis of a potential hybrid energy system, including such fees in the modeling is critical.

We neglect, also, the potential for the hybrid energy system to be co-located with a load. Depending upon prevailing tariff designs and incentive mechanisms, co-located load can affect the optimal design and operation of the hybrid energy system. For instance, some jurisdictions price energy consumption (*i.e.*, energy that is taken from the power system) differently to energy that is injected into the power system. Under such a pricing scheme, energy storage may be sized and operated to shape the net-load profile of the co-located hybrid energy system and load. Conversely, our modeling approach would apply if there is a net-metering tariff, which remunerates energy consumption and injections symmetrically. Another important consideration is that some jurisdictions offer incentive mechanisms for customers to self-supply energy. As an example, California’s Self Generation Incentive Program (SGIP) provides financial incentives for customers to self-supply energy.⁴ We do not consider SGIP or similar programs because our focus is understanding how retail pricing and the ITC incentivize the design and operation of hybrid energy systems. Consideration of incentive programs for self supplying energy would add another confounding variable to our analysis and is an area for future research. If co-located load is to be modeled, an approach, such as those that are developed by Besagni and Borgarello (2018); Brounen et al. (2012); Filippini and Pachauri (2004); Longhi (2015); Muratori et al. (2013) could be used to represent demand-side behavior.

Another important *caveat* of our work is that we do not account for the state of health, degradation, or cycle life of the energy storage in our model. Xi and Sioshansi (2016) incorporate a penalty on using energy storage that can capture the impact of cycling the energy-storage system on its eventual failure and replacement. Such an approach could be taken in our model. However, we do not believe that energy storage degradation would change markedly the distortionary impacts of prices, the ITC, and capacity payments.

Acknowledgments

The authors thank the editors, two anonymous reviewers, and Armin Sorooshian for helpful discussions and suggestions. Any opinions, conclusions, or errors that are expressed in this paper are solely those of the authors.

Appendix A. Linearization of Model

Optimization model (1)–(15) contains a number of nonlinearities, which occur due to decision variables being multiplied by one another. More specifically, (1) has terms in which τ is multiplied by \bar{I} , \bar{B}^P , and $\bar{B}^E \bar{B}^P$, the latter of which has two variables multiplied by one another. Constraint (13) has a term in which a piecewise-linear function of \bar{B}^E is multiplied by \bar{B}^P . Finally, (15) has a term in which τ is multiplied by P_t^C and $P_t^{PV,C}$.

These nonlinearities are linearized using binary expansion, which gives a linear approximation of the product, but requires the introduction of auxiliary binary variables. Sioshansi and Conejo (2017) detail the binary expansion method, which we outline here for an illustrative case of linearizing the bilinear term, $\pi = yz$, where both y and z are continuous variables. To apply binary expansion, we must approximate one of the two variables, which we take, without loss of generality, to be y , as taking on one of a finite set of values, which we denote as $\tilde{y}_1, \tilde{y}_2, \dots, \tilde{y}_m$. Then, we introduce a set of auxiliary variables, which we denote as $\zeta_1, \zeta_2, \dots, \zeta_n$, and approximate y as:

$$y \approx \sum_{i=1}^n \tilde{y}_i \zeta_i,$$

with the added restriction that:

$$\sum_{i=1}^n \zeta_i = 1. \tag{A.1}$$

⁴<https://www.cpuc.ca.gov/sgip/>

Because (A.1) allows exactly one of the ζ_i 's to equal 1, the corresponding value of \tilde{y}_i is the approximated value of y . With this approximation of y , we can approximate the original product as:

$$\pi \approx \sum_{i=1}^n \tilde{y}_i \zeta_i z. \quad (\text{A.2})$$

Each of the terms in the right-hand side of (A.2) involves the product of a binary and continuous variable. Each of these products can be linearized exactly by adding another continuous auxiliary variable. To demonstrate this, take the i th term from the right-hand side of (A.2), which is $\zeta_i z$. We must assume, further, that z has lower and upper bounds, which we denote as z^- and z^+ , respectively. We introduce a new auxiliary variable, which we denote as θ_i . We can represent the product using the conditions:

$$\begin{aligned} \zeta_i z &= z - \theta_i \\ -z^- \zeta_i &\leq \zeta_i z \leq z^+ \zeta_i \\ -z^- \cdot (1 - \zeta_i) &\leq \theta_i \leq z^+ \cdot (1 - \zeta_i). \end{aligned}$$

Combining all of these conditions implies that the bilinear term, $\pi = yz$, can be approximated linearly by adding the constraints:

$$\begin{aligned} \pi &= \sum_{i=1}^n \tilde{y}_i \cdot (z - \theta_i) \\ -z^- \zeta_i &\leq z - \theta_i \leq z^+ \zeta_i, \forall i = 1, \dots, n \\ -z^- \cdot (1 - \zeta_i) &\leq \theta_i \leq z^+ \cdot (1 - \zeta_i), \forall i = 1, \dots, n \\ \sum_{i=1}^n \zeta_i &= 1 \\ \zeta_i &\in \{0, 1\}, \forall i = 1, \dots, n; \end{aligned}$$

and the associated auxiliary variables, to the optimization problem in place of the original bilinear term. We apply this technique to linearize every bilinear term in (1), (13), and (15).

References

- Aneke, M., Wang, M., 1 October 2016. Energy storage technologies and real life applications—A state of the art review. *Applied Energy* 179, 350–377.
- Arbabzadeh, M., Johnson, J. X., Keoleian, G. A., August 2017. Parameters driving environmental performance of energy storage systems across grid applications. *Journal of Energy Storage* 12, 11–28.
- Arbabzadeh, M., Sioshansi, R., Johnson, J. X., Keoleian, G. A., 30 July 2019. The role of energy storage in deep decarbonization of electricity production. *Nature Communications* 10, 1–11.
- Besagni, G., Borgarello, M., 15 December 2018. The determinants of residential energy expenditure in Italy. *Energy* 165, Part A, 369–386.
- Bienstock, D., Muñoz, G., Yang, S., Matke, C., 12–15 December 2017. Robust linear control of storage in transmission systems, and extensions to robust network control problems. In: 2017 IEEE 56th Annual Conference on Decision and Control. Institute of Electrical and Electronics Engineers, Melbourne, Victoria, Australia, pp. 799–806.
- Blair, N., Dobos, A. P., Freeman, J., Neises, T., Wagner, M., Ferguson, T., Gilman, P., Janzou, S., February 2014. System Advisor Model, SAM 2014.1.14: General Description. Tech. Rep. NREL/TP-6A20-61019, National Renewable Energy Laboratory, Golden, CO.
- Brounen, D., Kok, N., Quigley, J. M., July 2012. Residential energy use and conservation: Economics and demographics. *European Economic Review* 56, 931–945.
- Chang, J., Karkatsouli, I., Pfeifenberger, J., Regan, L., Spees, K., Mashal, J., Davis, M., November 2014. The Value of Distributed Electricity Storage in Texas: Proposed Policy for Enabling Grid-Integrated Storage Investments. Tech. rep., The Brattle Group.
- Cole, W. J., Marcy, C., Krishnan, V. K., Margolis, R., 18–20 September 2016. Utility-scale Lithium-Ion Storage Cost Projections for Use in Capacity Expansion Models. In: 2016 North American Power Symposium. Institute of Electrical and Electronics Engineers, Denver, CO.

- Denholm, P., Eichman, J., Margolis, R., August 2017. Evaluating the Technical and Economic Performance of PV Plus Storage Power Plants. Tech. Rep. NREL/TP-6A20-68737, National Renewable Energy Laboratory, Golden, CO.
- Denholm, P., O'Connell, M., Brinkman, G., Jorgenson, J., November 2015. Overgeneration from Solar Energy in California: A Field Guide to the Duck Chart. Tech. Rep. NREL/TP-6A20-65023, National Renewable Energy Laboratory, Golden, CO.
- Denholm, P., Sioshansi, R., August 2009. The value of compressed air energy storage with wind in transmission-constrained electric power systems. *Energy Policy* 37, 3149–3158.
- Dunn, B., Kamath, H., Tarascon, J.-M., 18 November 2011. Electrical Energy Storage for the Grid: A Battery of Choices. *Science* 334, 928–935.
- Eyer, J. M., Corey, G., February 2010. Energy Storage for the Electricity Grid: Benefits and Market Potential Assessment Guide. Tech. Rep. SAND2010-0815, Sandia National Laboratories, Albuquerque, NM.
- Filippini, M., Pachauri, S., February 2004. Elasticities of electricity demand in urban Indian households. *Energy Policy* 32, 429–436.
- Fu, R., Feldman, D., Margolis, R., October 2018. U.S. Solar Photovoltaic System Cost Benchmark: Q1 2018. Tech. Rep. NREL/PR-6A20-72133, National Renewable Energy Laboratory, Golden, CO.
- Gallo, A. B., Simões-Moreira, J. R., Costa, H. K. M., Santos, M. M., Moutinho dos Santos, E., November 2016. Energy storage in the energy transition context: A technology review. *Renewable and Sustainable Energy Reviews* 65, 800–822.
- Habte, A., Sengupta, M., Lopez, A., April 2017. Evaluation of the National Solar Radiation Database (NSRDB Version 2): 1998–2015. Tech. Rep. NREL/TP-5D00-67722, National Renewable Energy Laboratory, Golden, CO.
- Hoppmann, J., Volland, J., Schmidt, T. S., Hoffmann, V. H., November 2014. The economic viability of battery storage for residential solar photovoltaic systems—A review and a simulation model. *Renewable and Sustainable Energy Reviews* 39, 1101–1118.
- Kintner-Meyer, M. C. W., Balducci, P., Colella, W., Elizondo, M. A., Jin, C., Nguyen, T., Viswanathan, V. V., Zhang, Y., June 2012. National Assessment of Energy Storage for Grid Balancing and Arbitrage: Phase 1, WECC. Tech. Rep. PNNL-21388, Pacific Northwest National Laboratory.
- Kyriakopoulos, G. L., Arabatzis, G., April 2016. Electrical energy storage systems in electricity generation: Energy policies, innovative technologies, and regulatory regimes. *Renewable and Sustainable Energy Reviews* 56, 1044–1067.
- Longhi, S., May 2015. Residential energy expenditures and the relevance of changes in household circumstances. *Energy Economics* 49, 440–450.
- Madaeni, S. H., Sioshansi, R., Denholm, P., January 2013a. Comparing Capacity Value Estimation Techniques for Photovoltaic Solar Power. *IEEE Journal of Photovoltaics* 3, 407–415.
- Madaeni, S. H., Sioshansi, R., Denholm, P., May 2013b. Estimating the Capacity Value of Concentrating Solar Power Plants with Thermal Energy Storage: A Case Study of the Southwestern United States. *IEEE Transactions on Power Systems* 28, 1205–1215.
- Mariaud, A., Acha, S., Ekins-Daukes, N., Shah, N., Markides, C. N., 1 August 2017. Integrated optimisation of photovoltaic and battery storage systems for UK commercial buildings. *Applied Energy* 199, 466–478.
- Muratori, M., Roberts, M. C., Sioshansi, R., Marano, V., Rizzoni, G., July 2013. A highly resolved modeling technique to simulate residential power demand. *Applied Energy* 107, 465–473.
- Sakti, A., Gallagher, K. G., Sepulveda, N., Uckun, C., Vergara, C., de Sisternes, F. J., Dees, D. W., Botterud, A., 28 February 2017. Enhanced representations of lithium-ion batteries in power systems models and their effect on the valuation of energy arbitrage applications. *Journal of Power Sources* 342, 279–291.
- Schmidt, O., Hawkes, A., Gambhir, A., Staffell, I., August 2017. The future cost of electrical energy storage based on experience rates. *Nature Energy* 2.
- Schoenung, S., April 2011. Energy Storage Systems Cost Update. Tech. Rep. SAND2011-2730, Sandia National Laboratories, Albuquerque, NM.
- Sengupta, M., Habte, A., Gotseff, P., Weekley, A., Lopez, A., Anderberg, M., Molling, C., Heidinger, A., September 2014a. A Physics-Based GOES Product for Use in NREL's National Solar Radiation Database. Tech. Rep. NREL/CP-5D00-62776, National Renewable Energy Laboratory, Golden, CO.
- Sengupta, M., Habte, A., Gotseff, P., Weekley, A., Lopez, A., Molling, C., Heidinger, A., July 2014b. A Physics-Based GOES Satellite Product for Use in NREL's National Solar Radiation Database. Tech. Rep. NREL/CP-5D00-62237, National Renewable Energy Laboratory, Golden, CO.
- Sengupta, M., Xie, Y., Lopez, A., Habte, A., Maclaurin, G., Shelby, J., June 2018. The National Solar Radiation Data Base (NSRDB). *Renewable and Sustainable Energy Reviews* 89, 51–60.
- Sioshansi, R., Conejo, A. J., 2017. *Optimization in Engineering: Models and Algorithms*. Vol. 120 of Springer Optimization and Its Applications. Springer Nature, Gewerbestraße 11, 6330 Cham, Switzerland.
- Sioshansi, R., Denholm, P., October 2010. The Value of Concentrating Solar Power and Thermal Energy Storage. *IEEE Transactions on Sustainable Energy* 1, 173–183.
- Sioshansi, R., Madaeni, S. H., Denholm, P., January 2014. A Dynamic Programming Approach to Estimate the Capacity Value of Energy Storage. *IEEE Transactions on Power Systems* 29, 395–403.
- Weniger, J., Tjaden, T., Quaschnig, V., 2014. Sizing of Residential PV Battery Systems. *Energy Procedia* 46, 78–87.
- Xi, X., Sioshansi, R., January 2016. A Dynamic Programming Model of Energy Storage and Transformer Deployments to Relieve Distribution Constraints. *Computational Management Science* 13, 119–146.
- Zafraakis, D., Chalvatzis, K. J., Baiocchi, G., Daskalakis, G., 15 December 2016. The value of arbitrage for energy storage: Evidence from European electricity markets. *Applied Energy* 184, 971–986.
- Zakeri, B., Syri, S., February 2015. Electrical energy storage systems: A comparative life cycle cost analysis. *Renewable and Sustainable Energy Reviews* 42, 569–596.

Zhu, D., Wang, Y., Chang, N., Pedram, M., 24-28 March 2014. Optimal Design and Management of a Smart Residential PV and Energy Storage System. In: 2014 Design, Automation & Test in Europe Conference & Exhibition. Institute of Electrical and Electronics Engineers, Dresden, Germany.